JOURNAL OF MATERIALS SCIENCE **34** (1999) 2401–2406

A study of the evolution of the constituent phases and magnetic properties of hydrogen-treated Sr-hexaferrite during calcination

N. MARTINEZ, A. J. WILLIAMS, S. A. SEYYED EBRAHIMI, I. R. HARRIS
School of Metallurgy and Materials, The University of Birmingham, Edgbaston, Birmingham, B15 2TT, UK

A hydrogen treatment followed by calcination, has been developed in order to enhance the intrinsic coercivity of Sr-hexaferrite ($SrFe_{12}O_{19}$). Fully hydrogen-treated Sr-hexaferrite consists of a mixture of 73%, by weight, of αFe and 27% of $Sr_7Fe_{10}O_{22}$ phases. Calcination of this material to reform the $SrFe_{12}O_{19}$ phase occurs in two stages. Between room temperature and 600 °C, oxygen was absorbed resulting in a large increase in weight with the formation of a mixture of $SrFeO_{3-x}$ and Fe_2O_3 (α and γ). During the second stage, the intermediate phases reacted to form $SrFe_{12}O_{19}$ at a temperature of between 700 and 800 °C. A partial desorption of oxygen occurred until calcination reached completion at 1000 °C. The magnetization at 1100 kA m^{-1} and the remanence were similar to those of the untreated material, but, because of a much refined grain size, the intrinsic coercivity was considerably larger, with values around 400 kA m^{-1}. Grain growth occurs at temperatures >1000 °C, resulting in a decrease in the intrinsic coercivity. © *1999 Kluwer Academic Publishers*

1. Introduction

A novel process, which consists of a treatment (in hydrogen, nitrogen or carbon) followed by calcination, has been established in order to enhance the intrinsic coercivity of Sr-hexaferrite [1]. This work showed that significant improvements were obtained with either conventionally or hydrothermally synthesized Sr-hexaferrite powders due to grain size refinement [2, 3]. Furthermore, if isotropic powder is required then one of the advantages of this new process is that the milling stage after conventional synthesis, widely used in the industrial production of ferrites, can be avoided [4].

During the hydrogen treatment, for instance, $SrFe_{12}O_{19}$ decomposes into a mixture that contains $Sr_7Fe_{10}O_{22}$, FeO and αFe [3]. However, the complete reduction of the Fe depends on the particular processing conditions, and optimum magnetic properties can be obtained when the H_2-treated material consists of only $Sr_7Fe_{10}O_{22}$ and αFe [4]. In the present study, the sequence of reactions involved in the production of the hexaferrite phase from the fully reduced mixture during the calcination stage has been determined.

2. Experimental procedure

In the present study, the initial Sr-hexaferrite material was supplied by Magnefabrik Schramberg (Germany), and consisted of black, unmilled, spherical agglomerates of powder. The composition was the stoichiometric $SrO \cdot 6Fe_2O_3$ compound. The material was treated in a flow of hydrogen at 700 °C for 3 h [4]. One of the hydrogen-treated agglomerates was retained as a reference. The final calcination stage consisted of heating the samples in air at 5 °C min^{-1} in a muffle furnace. The samples were taken out of the furnace at temperatures of between 100 and 1200 °C. It was assumed that the composition was stable when the samples were cooled from the calcination temperature to room temperature in air.

The weight of every sample was measured before and after the calcination treatment in order to determine the weight change, Δm, with respect to an uncalcined sample.

The magnetic properties, such as intrinsic coercivity, remanence and magnetization at 1100 kA m^{-1}, were measured at room temperature with a vibrating sample magnetometer (VSM) on magnetically unaligned solid or powdered samples. The VSM measurements were not corrected for self-demagnetizing factors. Crushing was not necessary for the samples that were calcined to 100, 200, 300 and 350 °C, as these samples consisted of solid agglomerates. The samples that were calcined to temperatures higher than 400 °C were friable, and the VSM samples were produced by hand-crushing with a mortar and pestle and then setting in molten wax.

The phases within the samples were identified by X-ray diffraction (XRD) analyses using CoK_α radiation on powdered samples. The intensity was normalized to 100% with respect to the most intense peak. The XRD patterns were indexed using JCPDS cards. No significant diffraction peaks were obtained from phases that represented less than 10%, by volume, of the samples.

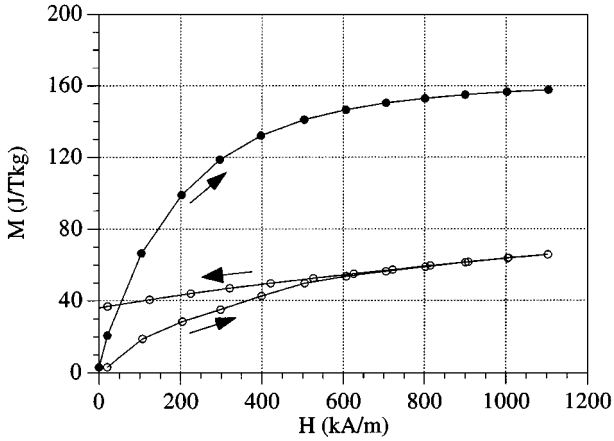

Figure 1 VSM traces of an "as-received ball" and after optimum H_2-treatment (—•—): M, magnetization; H, applied field.

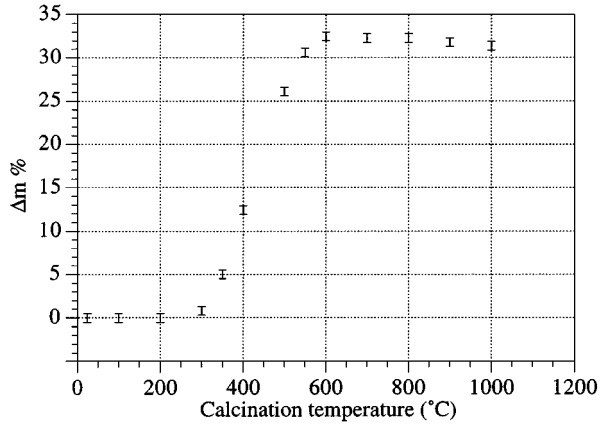

Figure 2 Variation in weight, Δm, with calcination temperature.

3. Results and discussion

3.1. Hydrogen-treated material

The optimally hydrogen-treated material still consisted of the original spherical agglomerates, but they now had a greenish/brown colour. The initial material exhibited isotropic magnetic properties with an intrinsic coercivity of 281 ± 8 kA m^{-1}, a remanence of 35.9 ± 2 J T^{-1} kg^{-1} and a magnetization at 1100 kA m^{-1} of 66 ± 2 J T^{-1} kg^{-1}. The optimally hydrogen-treated material exhibited a much larger magnetization at 1100 kA m^{-1}, of 158 ± 2 J T^{-1} kg^{-1} (Fig. 1), as reported by Ataie *et al*. [1, 2]. Furthermore, both the intrinsic coercivity (approximately 3 ± 8 kA m^{-1}) and the remanence (3 ± 2 J T^{-1} kg^{-1}) were very low compared with those of the starting material. This change in magnetic properties was attributed to the decomposition of $SrFe_{12}O_{19}$ into a mixture containing a high proportion of αFe [3].

XRD analyses showed that the H_2-treated material consisted of αFe and $Sr_7Fe_{10}O_{22}$ phases (see the room temperature (r.t.) XRD pattern in Fig. 3). No FeO phase was identified, indicating a further degree of decomposition compared with the study described by Ebrahimi *et al*. [3]. The complete decomposition can be summarized by Equation 1

$$7(SrO \cdot 6Fe_2O_3) + 111H_2 \rightarrow 7(SrO \cdot 5Fe_2O_3) + 74\alpha Fe + 111H_2O_{(g)} \quad (1)$$

which also indicates that the proportions should be approximately 73%, by weight, of αFe and approximately 27% of $Sr_7Fe_{10}O_{22}$. As the $Sr_7Fe_{10}O_{22}$ phase is paramagnetic then the ferromagnetic properties of the H_2-treated material can be attributed to αFe. Therefore, the proportion of αFe in the mixture can also be estimated by comparing the magnetization at 1100 kA m^{-1} with the saturation magnetization of pure αFe ($\sigma_s = 218$ J T^{-1} kg^{-1} at 20 °C [5]). The estimated value is approximately 73%, by weight, and this is in excellent agreement with the value calculated from Equation 1.

3.2. Calcination

The samples that were calcined to 100, 200, 300 and 350 °C still had the greenish/brown colour and spherical shape, of the H_2-treated samples. However, the samples that were calcined to temperatures >400 °C were black and friable. Equation 2 summarizes the complete calcination stage

$$Sr_7Fe_{10}O_{22} + 74\alpha Fe + 55.5O_2 \rightarrow 7SrFe_{12}O_{19} \quad (2)$$

3.2.1. Weight changes

According to Equation 2, the weight increase on complete calcination was estimated to be 31.4%. Fig. 2 shows the variation in weight with the calcination temperature. No change was observed between r.t. and 200 °C, indicating that the mixture of αFe and $Sr_7Fe_{10}O_{22}$ was stable within this temperature range, while heating at 5 °C min^{-1}. A large increase occurred between 200 and 600 °C resulting in a total increase of +32.5%. From 600 to 1000 °C, the relative weight decreased gradually to 31.4%, which is in excellent agreement with the value obtained from Equation 2. This behaviour shows that calcination did not consist of a single reaction as represented in Equation 2 but consisted of, at least, two stages.

3.2.2. Evolution of the constituent phases

Fig. 3 shows the XRD patterns of the samples from the H_2-treated sample (r.t.) to the fully calcined sample. Only the patterns of the samples that had different phase compositions are represented. The expected phases, which are αFe (cubic [6]), $Sr_7Fe_{10}O_{22}$ (orthorhombic [7, 8]) and $SrFe_{12}O_{19}$ (hexagonal [9]), were identified. However, intermediate phases were also found. These were $SrFeO_{3-x}$ (cubic [10]), and two types of Fe_2O_3, maghemite (γ, tetragonal [11]) and hematite (α, rhombohedral [12]). The existence of intermediate products shows that calcination is a multistage process, as suggested above by the weight changes. This process can be compared with the two-stage calcination of $SrCO_3$ and αFe_2O_3 to produce $SrFe_{12}O_{19}$. This process was characterized by Haberey and Kockel [10], who reported the existence of the intermediate phase $SrFeO_{3-x}$ (with perovskite structure) above 660 °C in air. They also observed the formation of the $SrFe_{12}O_{19}$ phase at 810 °C, and concluded that the formation of this phase from pure $SrCO_3$ with six parts of αFe_2O_3,

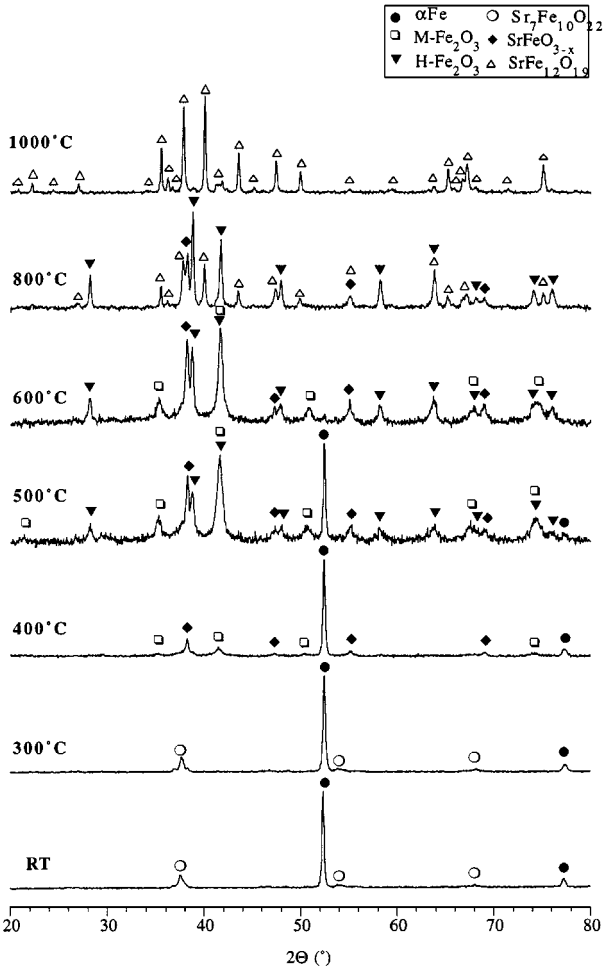

Figure 3 XRD patterns of Sr-hexaferrite samples that were first hydrogen treated and then calcined by heating at 5 °C min^{-1} up to the temperature indicated.

in air, proceeded partially or totally via the intermediate phase, $SrFeO_{3-x}$.

The XRD pattern of the sample obtained at 300 °C is the same as that of the fully reduced material (r.t.). Nevertheless, the weight had increased by 0.8% showing that the sample had started to react with air, but the proportion of the new phase(s) was too small to be identified by XRD.

Some maghemite was identified in the diffraction pattern of the sample obtained at 350 °C. The maghemite phase, γFe_2O_3, was reported to be metastable above 300 °C with respect to the hematite phase, αFe_2O_3. However, according to Takei and Chiba [13], maghemite can be stabilized up to a temperature of approximately 700 °C when grown on an appropriate substrate. In the present study, it was identified in the samples calcined to temperatures of between 350 and 700 °C, suggesting that this phase might be stabilized by another phase. The peak intensities of γFe_2O_3, relative to αFe, increased from 350 to 550 °C. At 400 °C, the predominant Sr-containing phase changed from $Sr_7Fe_{10}O_{22}$ to $SrFeO_{3-x}$. The hematite phase (αFe_2O_3) was first identified at 500 °C.

The (1 1 0) peak of αFe was the most intense in the XRD patterns of the samples, which were calcined to temperatures of between 100 and 500 °C, but was relatively weak in that of the sample which was calcined to 550 °C. No αFe was identified in the 600 °C sample, indicating that most of it had completely disappeared. Fig. 2 indicated a maximum in the weight gain for the sample that was calcined to 600 °C. This result might indicate that αFe was fully oxidized into Fe_2O_3 (α and γ). Although it is probable that at least two reactions occur concurrently between approximately 300 and 600 °C, the reaction can be summarized by Equation 3. The corresponding increase in weight would be 32.4% (assuming $x = 0$ in $SrFeO_{3-x}$), which is in very good agreement with the experimental value obtained at 600 °C. Thus, $SrFeO_{3-x}$ represents approximately 18%, by weight, and Fe_2O_3 82% in the mixture.

Between r.t. and 600 °C

$$Sr_7Fe_{10}O_{22} + 74\alpha Fe + \frac{(114.5 - 7x)}{2}O_2 \rightarrow 7SrFeO_{3-x} + 38.5Fe_2O_3 \quad (3)$$

The (1 1 9) γFe_2O_3 peak was the most intense between 550 and 700 °C. The sample that was calcined to 700 °C gave an XRD pattern similar to that of the sample which was calcined to 600 °C. This might indicate that no further reaction happened between 600 and 700 °C, unless the proportion of new product(s) was too small to be detected. No maghemite was identified and the αFe_2O_3 (1 2 1) peak was most intense in the sample that was calcined to 800 °C. This observation suggested that maghemite may have either reacted to form $SrFe_{12}O_{19}$ or transformed into hematite. The Sr-hexaferrite phase was identified in samples that were calcined to 800, 900 and 1000 °C, and the intensity of the $SrFe_{12}O_{19}$ peaks indicated that the proportion of this phase increased with increasing calcination temperature at the expense of the $SrFeO_{3-x}$ and αFe_2O_3 phases. Therefore, it appears that $SrFeO_{3-x}$ and αFe_2O_3 react, with a loss of oxygen, to produce $SrFe_{12}O_{19}$, as shown in Equation 4

$$SrFeO_{3-x} + 5.5\alpha Fe_2O_3 \rightarrow SrO \cdot 6Fe_2O_3 + \frac{(0.5 - x)}{2}O_2 \quad (4)$$

In addition, the weight change showed a small decrease from 600 to 1000 °C related to the small loss of oxygen. These observations indicate that the reaction is the "B-step" given by Haberey and Kockel [10]. Only the Sr-hexaferrite phase was identified in the samples that were calcined to 1100 and 1200 °C.

3.2.3. Magnetic properties

The magnetic properties of iron and its different iron oxides, which were identified in this study, were obtained from the literature. Alpha iron is ferromagnetic and exhibits a saturation magnetization of 218 J T^{-1} kg^{-1} at 20 °C [5]. Hematite (αFe_2O_3) is antiferromagnetic at r.t. with a weak ferromagnetism that persists up to 680 °C [14], its saturation magnetization is much lower than that of αFe, with a value of 0.4 J T^{-1} kg^{-1}, and its intrinsic coercivity is approximately 0.52 ± 0.08 kA m^{-1} [15]. Maghemite (γFe_2O_3) is ferrimagnetic and has a saturation magnetization of

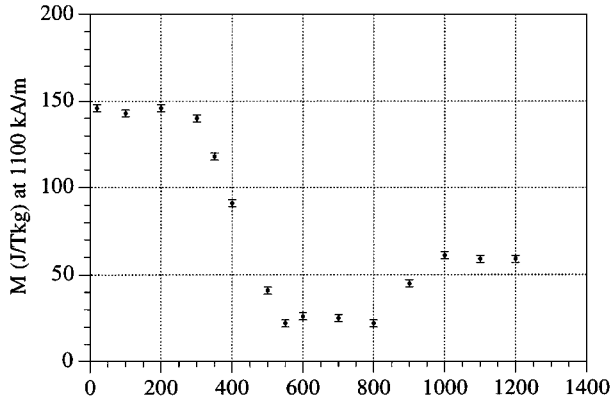

Figure 4 Changes in magnetization at 1100 kA m^{-1} with calcination temperature (°C).

approximately 83 J T^{-1} kg^{-1} [13]. Finally, according to Shimony and Knudsen [16], $SrFeO_{3-x}$ is paramagnetic at room temperature.

3.2.3.1. Saturation magnetisation. Fig. 4 shows the variation of magnetization at 1100 kA m^{-1} with calcination temperature. The initial value (146 ± 2 J T^{-1} kg^{-1}) was lower than that given in Section 3.1 (158 ± 2 J T^{-1} kg^{-1}) showing some evidence of partial oxidation at r.t. in air since the sample from Section 3.1 was measured within a week after the H_2-treatment (representative value) and the series of calcinations were carried out a month later. However, the proportion of oxide formed was too small to be identified by XRD analysis under the conditions used. Since the only magnetic phase in the H_2-treated mixture is αFe, the decrease in magnetization was probably due to the partial oxidation of Fe.

The samples calcined to 100 and 200 °C exhibited a large saturation magnetization (approximately 150 J T^{-1} kg^{-1}), comparable with that of the uncalcined sample, indicating that no significant change in composition occurred. This is in agreement with the weight change and XRD analyses.

The magnetization at 1100 kA m^{-1} started to decrease after calcination up to 300 °C indicating that some reactions had started. A significant decrease in M occurred between 300 and 550 °C due to the disappearance of αFe and the formation of iron oxides, both α- and γFe_2O_3, which have much lower magnetization than that of αFe. The samples that were calcined to between 550 and 800 °C exhibited low values of magnetization (approximately 25 J T^{-1} kg^{-1}) because of the large proportions of iron oxides. The magnetization increased from 800 to 1000 °C because of the formation of $SrFe_{12}O_{19}$ and the disappearance of hematite. It remained constant between 1000 and 1200 °C because calcination had reached completion, and M was the same as that of the starting material (approximately 65 ± 2 J T^{-1} kg^{-1}).

3.2.3.2. Intrinsic coercivity and remanence. The samples that were calcined to 100 and 200 °C exhibited intrinsic coercivities and remanences comparable with those of the H_2-treated sample (Fig. 5). This is because no significant change in phase composition had occurred, as indicated by the weight change measurements and magnetization at 1100 kA m^{-1}.

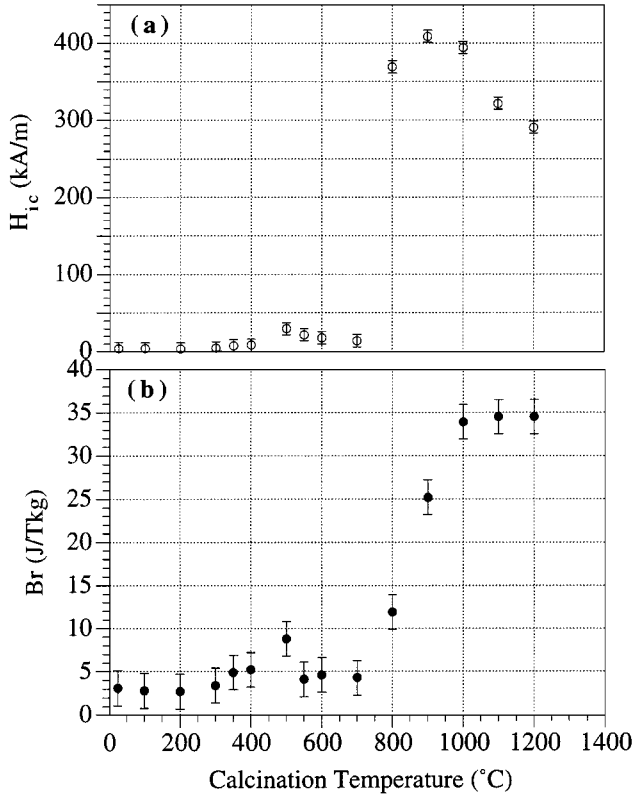

Figure 5 Changes in intrinsic coercivity, H_{IC}, (a), and remanence, Br (b), with calcination temperature.

After a calcination up to temperatures between 300 and 700 °C, the samples had slightly larger intrinsic coercivities and remanences than those of the samples that were calcined to temperatures below 200 °C. Although these changes are within the experimental error, maximum values were obtained for the samples calcined to 500 °C. This might indicate that both magnetic properties were constant between r.t. and 200 °C, increased slightly from 300 to 500 °C and decreased from 500 to 700 °C. This temperature range corresponds to that where a dramatic weight increase occurred and both iron oxides (maghemite and hematite) were formed. Thus the magnetic properties of these samples depend on the proportions of αFe, αFe_2O_3 and γFe_2O_3. At r.t., the intrinsic coercivity and remanence of γFe_2O_3 are significantly larger than those of αFe and αFe_2O_3. In the sample calcined to 400 °C, the magnetic properties are due to αFe and γFe_2O_3; the relative intensities shown in the XRD pattern indicate that the proportion of αFe is much larger than that of maghemite and hence the coercivity and remanence are similar to that of the samples containing just αFe and $Sr_7Fe_{10}O_{22}$. According to the XRD pattern, the sample that was calcined to 500 °C, contained αFe, αFe_2O_3 and γFe_2O_3, and the proportion of maghemite was comparable with that of αFe and significantly larger than that of hematite. This result suggested that between 400 to 500 °C, the amount of maghemite and hematite increased at the

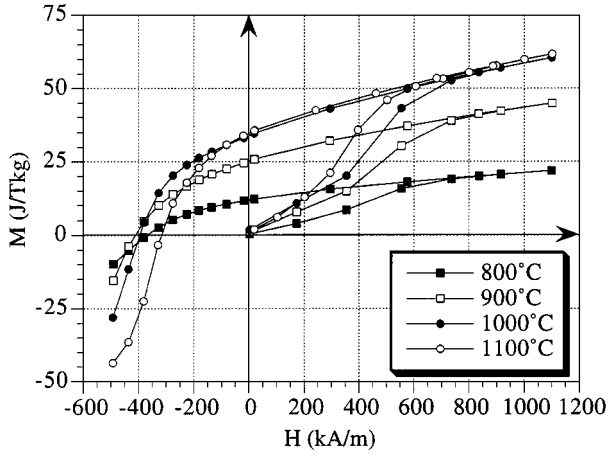

Figure 6 VSM traces of the samples calcined between 800 and 1100 °C: H, applied field, M, magnetization.

expense of αFe. It appears therefore, that the proportion of maghemite in the sample was large enough to enhance both the coercivity and the remanence. The sample that was calcined to 600 °C contained both iron oxides but no Fe, and the relative intensities on the XRD pattern showed similar proportions of both maghemite and hematite. Therefore, the decrease in remanence and intrinsic coercivity can be ascribed to the increased hematite content.

Both properties increased drastically when the samples were calcined to a temperature $\geq$800 °C due to formation of the $SrFe_{12}O_{19}$ phase. Fig. 6 represents the VSM traces of the samples calcined to temperatures between 800 and 1100 °C. The initial magnetization curves indicated that the coercivity was controlled by the presence of single domain particles. The intrinsic coercivities were much larger than that of the initial material because of the submicrometre grain size [2]. However, the remanences of both the samples calcined to 800 and 900 °C were lower than those of the samples that were calcined to temperatures $\geq$1000 °C. This was attributed to the fact that the former were not single phase and hence the $SrFeO_{3-x}$ and αFe_2O_3 phases acted to dilute the remanence. The sample that was calcined to 900 °C exhibited the largest intrinsic coercivity, which might be due to the magnetic isolation provided by these secondary phases. The remanence became constant with calcination to temperatures $\geq$1000 °C, as did the magnetization at 1100 kA m^{-1}, because the samples were single phase. On the other hand, the intrinsic coercivity decreased from 1000 to 1200 °C probably because of grain growth at these temperatures. This can be deduced from the initial magnetization curves represented in Fig. 6, where the initial magnetization curves became progressively steeper over this temperature range.

The present work shows that optimum calcination is achieved by heating at 5 °C min^{-1} to a temperature of 1000 °C, which is a compromise of coercivity and remanence. This is in agreement with previous work on this subject [3] carried out in these laboratories. The magnetic properties of the optimally processed sample were isotropic, as were those of the initial material, with the same remanence values and magnetization at 1100 kA m^{-1} values, but with a much enhanced intrinsic coercivity.

4. Conclusions

Fully hydrogen-treated Sr-hexaferrite consists of a mixture of 73%, by weight, of αFe and 27% of $Sr_7Fe_{10}O_{22}$ phases, and exhibits a high saturation magnetization and low intrinsic coercivity and remanence due to the large proportion of αFe. Calcination of this material to reform the $SrFe_{12}O_{19}$ phase occurs in two main stages. Between 300 and 600 °C, oxygen is absorbed resulting in a weight increase of 32.5%, and a mixture of 18%, by weight, of $SrFeO_{3-x}$ and 82% of Fe_2O_3 (α and γ). The magnetization at 1100 kA m^{-1} decreases dramatically because of the formation of iron oxides at the expense of αFe. The intrinsic coercivity and remanence remain low, compared with those of the Sr-hexaferrite phase, because of the poor permanent magnetic properties of αFe, hematite and maghemite. During the second stage, the intermediate phases start reacting to form $SrFe_{12}O_{19}$ at a temperature of between 700 and 800 °C. A partial desorption of oxygen occurs when calcination has reached completion at 1000 °C and the final weight increase, relative to the hydrogen-treated material, is 31.4%. The magnetization at 1100 kA m^{-1}, intrinsic coercivity and remanence increase with the formation of the hexaferrite phase. The magnetization at 1100 kA m^{-1} and remanence are similar to those of the untreated material (as-received), but the intrinsic coercivity is considerably larger, with values around 400 kA m^{-1}, because of a much refined grain size. Grain growth occurs at temperatures >1000 °C, resulting in a decrease in intrinsic coercivity. The complete process investigated in this work is summarized in Fig. 7.

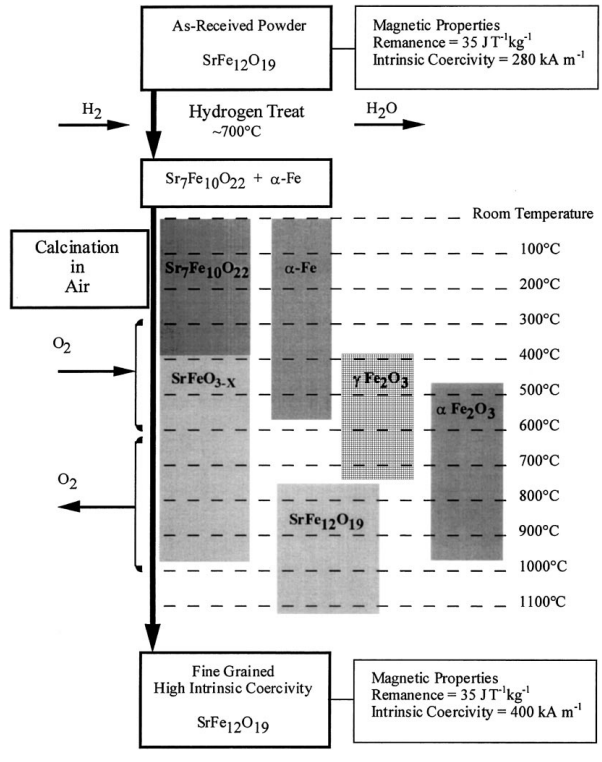

Figure 7 Summary of reactions occurring during hydrogen treatment and calcination.

Acknowledgements

The authors would like to thank Dr B. Grieb of Magnefabrik Schramberg (Germany) for providing the material, and Drs R. V. Major, R. J. Freeman and D. Kendall of Telcon plc (UK) for providing gas-treatment facilities.

References

1. A. ATAIE, C. B. PONTON and I. R. HARRIS, Patent PCT/GB95/02758, November (1995).
2. *Idem*, *J. Mater. Sci*. **31** (1996) 5521.
3. S. A. S. EBRAHIMI, A. J. WILLIAMS, N. MARTINEZ, A. ATAIE, A. KIANVASH, C. B. PONTON and I. R. HARRIS, *J. De Physique IV*, **7 (C1)** (1997) 325.
4. A. J. WILLIAMS, N. MARTINEZ, A. ROGERS and I. R. HARRIS, to be published.
5. B. D. CULLITY, "Introduction to Magnetic Materials" (Addison-Wesley, Philippines, 1972).
6. H. E. SWANSON, *Natl. Bur. Stand*. **4** (1955) 3; JCPDS 06-0696.
7. R. BRISI, *Ann. Chim*. **59** (1969) 385; JCPDS 22-1427.
8. E. LUCCHINI, D. MINICHELLI and G. SLOCCARI, *J. Amer. Ceram. Soc*. **57** (1974) 42; JCPDS 26-0980.
9. V. ADELSKOLD, *Arkiv for Kemi, Mineralogioch Geologi*, **12A** (1938) 1.
10. F. HABEREY and A. KOCKEL, *IEEE Trans. Magn*. **Mag-12** (1976) 983; JCPDS/34-0638.
11. G. BROWN, "The X-Ray Identification and Crystal Structures of Clay Minerals" (London: Mineralogical Society, 1961); JCPDS/25-1402.
12. V. KASTALSKY and M. F. WESTCOTT, *Aust. J. Chem*. **21** (1968) 1061; JCPDS/13-0534.
13. H. TAKEI and S. CHIBA, *J. Phys. Soc. Jpn* **21** (1966) 1255.
14. S. FREIER, M. GREENSHPAN, P. HILLMAN and H. SHECHTER, *Phys. Lett*. **2** (1962) 191.
15. P. J. FLANDERS and J. P. REMEIKA, *Phil. Mag*. **11** (1965) 1271.
16. U. SHIMONY and J. M. KNUDSEN, *Phys. Rev*. **144** (1966) 361.

Received 6 April
and accepted 3 September 1998